# Faraday Discussions

Accepted Manuscript


This manuscript will be presented and discussed at a forthcoming Faraday Discussion meeting. All delegates can contribute to the discussion which will be included in the final volume.

**Register now to attend!** Full details of all upcoming meetings: http://rsc.li/fd-upcoming-meetings

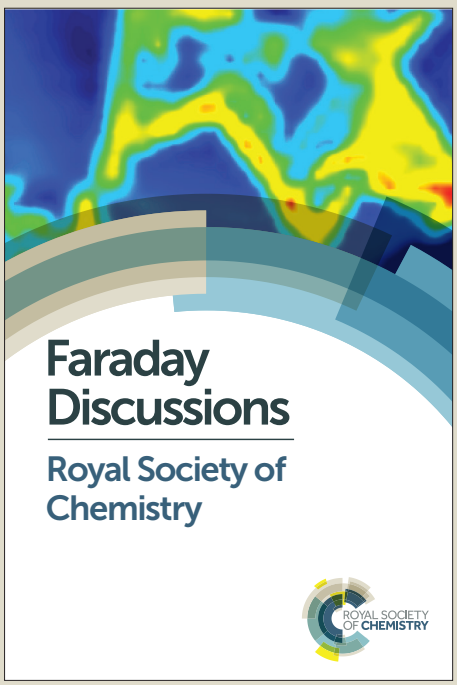


This is an *Accepted Manuscript*, which has been through the Royal Society of Chemistry peer review process and has been accepted for publication.

*Accepted Manuscripts* are published online shortly after acceptance, before technical editing, formatting and proof reading. Using this free service, authors can make their results available to the community, in citable form, before we publish the edited article. We will replace this *Accepted Manuscript* with the edited and formatted *Advance Article* as soon as it is available.

You can find more information about *Accepted Manuscripts* in the Information for Authors.

Please note that technical editing may introduce minor changes to the text and/or graphics, which may alter content. The journal's standard Terms & Conditions and the Ethical guidelines still apply. In no event shall the Royal Society of Chemistry be held responsible for any errors or omissions in this *Accepted Manuscript* or any consequences arising from the use of any information it contains.

ROYAL SOCIETY OF CHEMISTRY

www.rsc.org/faraday_d

# Electron Transport in All-Carbon Molecular Electronic Devices

Richard McCreery[1,2], Adam Bergren[2],
Amin Morteza-Najarian[1,2], Sayed Nagy[1,2], Haijun Yan[2]

[1]Department of Chemistry
University of Alberta
[2]National Institute for Nanotechnology
11421 Saskatchewan Drive
Edmonton, Alberta T6G 2M9
Canada

**Abstract**

Carbon has always been an important electrode material for electrochemical applications, and the relatively recent development of carbon nanotubes and graphene as electrodes has significantly increased interest in the field. Carbon solids, both $sp^2$ and $sp^3$ hybridized, are unique in their combination of electronic conductivity and the ability to form strong bonds to a variety of other elements and molecules. The Faraday Discussion included broad concepts and applications of carbon materials in electrochemistry, including analysis, energy storage, materials science, and solid-state electronics. This introductory paper describes some of the special properties of carbon materials useful in electrochemistry, with particular illustrations in the realm of molecular electronics. The strong bond between $sp^2$ conducting carbon and aromatic organic molecules enables not only strong electronic interactions across the interface between the two materials, but also provides sufficient stability for practical applications. The last section of the paper discusses several factors which affect the electron transfer kinetics at highly ordered pyrolytic graphite, some of which are currently controversial. These issues bear on the general question of how the structure and electronic properties of the carbon electrode material control its utility in electrochemistry and electron transport, which are the core principles of electrochemistry using carbon electrodes.

## 1. Introduction

Carbon electrodes have been prominent in electrochemistry since the days of Faraday himself, particularly for anodic reactions not possible on mercury due to its relative ease of oxidation. Carbon is essential for operation of the home glucose analyser, which is arguably the most performed chemical analysis in history, certainly in the past several decades. The discovery of the fullerenes, including carbon nanotubes and graphene, significantly raised the profile of carbon materials in areas beyond electrochemistry, as did the development of vapour deposited conducting diamond electrodes. As will be discussed in later sections, the electronic properties of carbon as well as its ability to form a variety of strong bonds with organic molecules distinguish carbon electrodes from metals and other materials, and underlie many of their useful applications. The Faraday Discussion and associated manuscripts reveal the "many faces" of both $sp^2$ and $sp^3$carbon electrode materials, with broad applications in energy conversion, electroanalysis, electronics, and bioanalytical chemistry. The advent of carbon nanotubes and graphene has stimulated renewed interest in electrochemical applications of novel carbon materials, as reflected in several of the contributed manuscripts. While several of the papers presented at this Faraday Discussion deal directly with fullerenes in electrochemistry, they will not be addressed in this introductory paper. In addition to an overview of some of the special properties of carbon electrodes, this chapter will describe extensions of electrochemical concepts to the area of molecular electronics, where carbon electrodes have both fundamental and practical advantages. The unique property of $sp^2$ (or $sp^3$) hybridized carbon as electronic conductors capable of a wide variety of covalent surface modifications is particularly valuable for providing "contact" between a conductor and an aromatic organic molecule. A practical application of carbon-based molecular electronics in audio processing will be described briefly,

followed by a discussion of some recent controversy regarding the electrochemical behaviour of highly ordered pyrolytic graphite electrodes.

**2. Special properties of carbon materials as electrodes**

As is well known, carbon materials can exhibit high electronic conductivity, either intrinsically in graphite or glassy carbon, or in diamond doped with boron, nitrogen, etc. [1, 2] Furthermore, the rich covalent chemistry of carbon is the basis of nearly all organic and biochemistry, with a wide variety of bonding to many other elements. The often-cited advantages of both $sp^2$ and $sp^3$ carbon solids for electrochemistry include wide potential window, mainly due to slow kinetics for the oxidation of the carbon itself, as well as low cost and widespread availability in many distinct forms. Metal electrode surfaces can be modified with a variety of chemisorbed and physisorbed molecular mono- and multilayers, but in many cases these modifications are unstable to temperature, time, and potential excursions. The properties of a metal-carbon bond depend strongly on the metal involved, whereas the C-C bond between a conducting $sp^2$ or $sp^3$ carbon solid is nearly always strong, and able to survive elevated temperatures and many reactive conditions. An example of a modified carbon electrode is shown in figure 1A, for the case of an aromatic molecule bonded to a $sp^2$ hybridized carbon surface via diazonium reduction [3, 4].

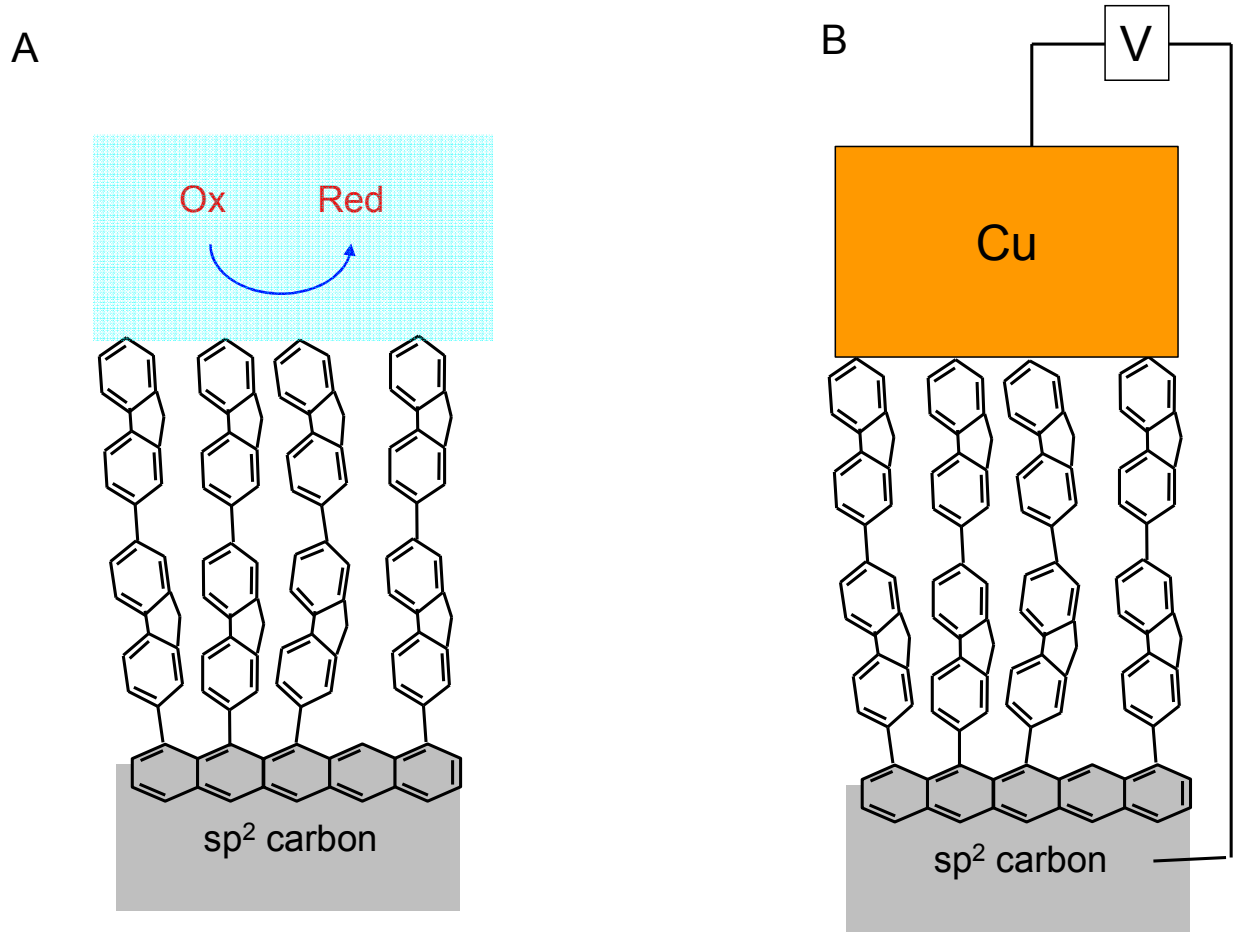


**Figure 1**. Schematics of modified $sp^2$ carbon surfaces consisting of aromatic molecules covalently bonded to edge sites of a conducting carbon solid, used as a modified electrode in solution (A) or in a molecular junction (B).

As already noted, modified carbon electrodes using glucose oxidase and related cofactors are the basis of the home glucose sensor used by a large fraction of the world's diabetics. The C-C surface bond shown in figure 1A is stable to sonication, acid or base treatment, most organic solvents, and temperatures above 400 $^{o}$C in a vacuum [3, 5-7].

An important carbon fabrication technique for electronics applications is pyrolysis of photoresist polymers to form "pyrolyzed photoresist films" (PPF) [8-11]. The process is shown schematically in figure 2, starting with standard silicon wafers and commercial photoresist materials. Photoresist is often a phenolic resin (e.g. "novolac") which is designed to spin coat

evenly on silicon, often coated with native or thermal oxide. A photosensitizer permits patterning of the resist by conventional photolithography if desired, then the wafer is heat treated in a 5% $H_2$/95% $N_2$ atmosphere. The result is a very flat (<0.5 nm rms by AFM) mainly $sp^2$ carbon surface, with conductivity similar to that of glassy carbon. PPF has been used to make a variety of carbon nanostructures, many of which have been used for electrochemistry.

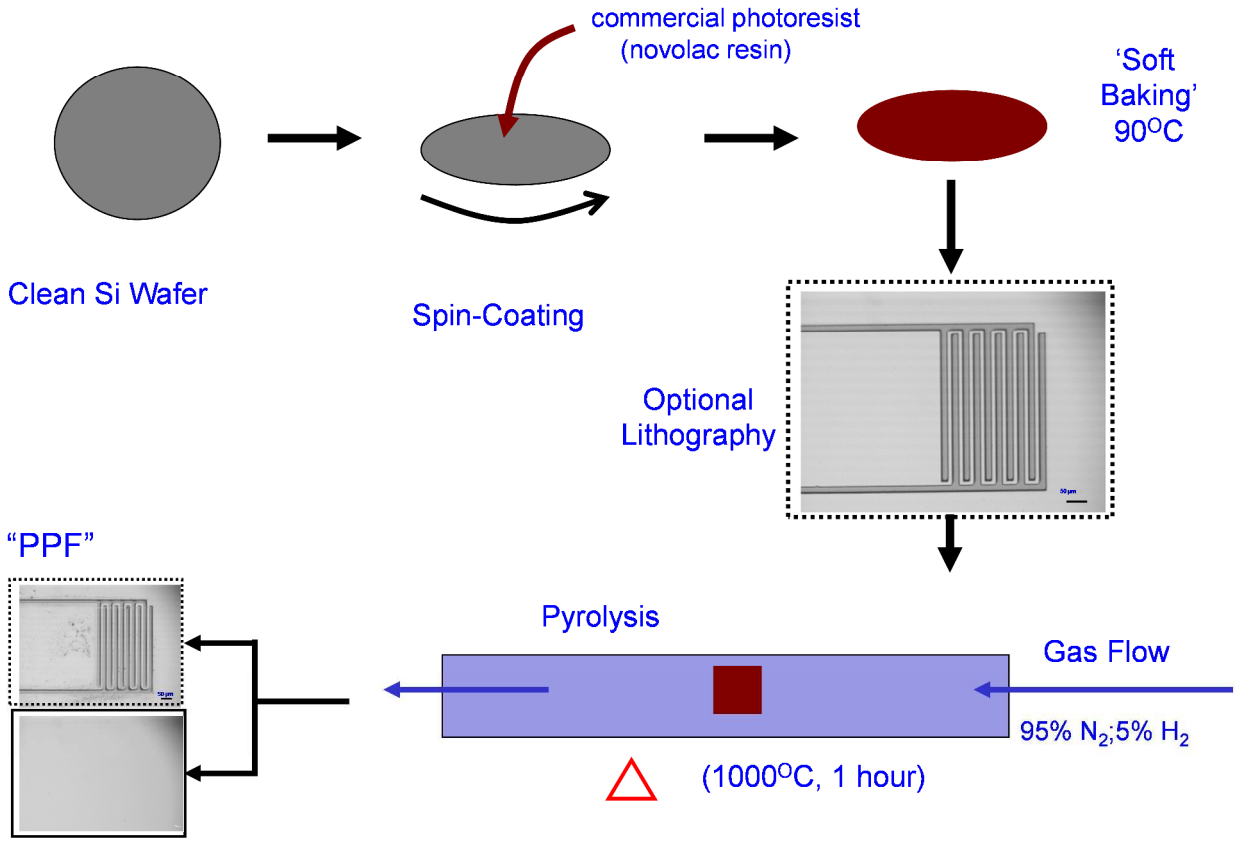


**Figure 2**. Formation of pyrolyzed photoresist film (PPF) from a positive photoresist to make either "blanket" or patterned $sp^2$ hybridized carbon films on Si/SiOx surfaces. Surface exhibits and rms roughness < 0.4 nm, measured by AFM.

The electrochemical properties of PPF are similar to those of glassy carbon, but its low oxide coverage results in weaker adsorption, and the observed electron transfer rates are generally lower than those of glassy carbon [10]. Reduction of diazonium reagents on PPF results in modified electrodes with high coverage, but often forms multilayers by subsequent radical attack of the

initial modification layer [12, 13]. While the layer thickness can be controlled by the electrochemical conditions, it should be verified with AFM "scratching" [14]. Since the PPF surface is disordered and contains a mixture of edge and basal sites, the bonding geometry is difficult to determine, although the more rapid reaction of diazonium reagents on step edge defects [13] implies that the majority of the surface bonding is between $sp^2$ edges on the PPF and an aromatic ring from the diazonium reagent, as shown in figure 1A. While modification of the basal plane of graphitic surfaces is possible[15, 16], the resulting disruption of three aromatic rings likely makes the reaction slower than on edge plane.

Electron-beam deposited carbon is another relative newcomer to the field, and can be useful in electronics applications [17-20]. E-beam deposition is widely used for metals and refractory materials, and is based on an energetic electron beam striking a target in high vacuum ($< 10^{-6}$ torr). Atoms and clusters are generated at the target, which travel to a sample surface where they deposit, possibly with subsequent diffusion [21, 22]. When graphite rods are used as a target, the resulting beam of carbon atoms and clusters forms a flat, conformal film on the sample (designated e-Carbon, or e-C). Since carbon atoms and clusters are very reactive, diffusion is unlikely after deposition. Surprisingly, the Raman spectrum of a diazonium-derived molecular layer shows no change in relative intensities after e-C deposition, implying minor modifications to the molecular layer, if any[20]. Although the conductivity of e-C is much lower than that of PPF, the e-C layer may be sufficiently thin (<20 nm) that its Ohmic resistance is often negligible along the axis perpendicular to the layer surface. E-beam deposition of either Cu or e-C "top contacts" completes the molecular junction (MJ), as shown schematically in figure 1B. A thin layer of e-C (2-5 nm) may also be deposited on the molecular layer to prevent subsequent penetration of metals such as Au into the molecular layer[20]. For e-C, Cu, or Au

deposition, no changes were observed in the Raman spectrum after deposition, although Ti and Pt caused significant changes in relative and absolute peak intensities, indicating damage of the molecular layer [23]. The "all carbon" molecular junction consisting of an organic molecular layer between PPF and e-C (or two films of e-C) has some special advantages due to the stability of carbon and its resistance to oxidation and electromigration, which cause failure of PPF/molecule/Cu devices at high bias [20, 24].

**3. Carbon-based Molecular Electronics**

The MJ structure in figure 1B indeed turns the molecular layer into a circuit component[5, 6, 25, 26], but in contrast to the modified electrode, there is no solvent, mobile ions, ionic double layer, or mass transport. Furthermore, there is no reference electrode as in conventional electrochemistry, hence the relevant potential scale is usually referred to the vacuum level. An electron at the Normal Hydrogen Electrode (NHE) potential has a Fermi energy of -4.5 V relative to a vacuum[27], while a typical molecular HOMO level has an energy of -6 V relative to vacuum. The relationship between redox potentials and the vacuum level is rather complex, but the relative energies of molecular orbitals compared to the contact Fermi level are critical to determining junction behaviour. For the current discussion, suffice it to say that comparisons of energetics in a MJ with the electrochemical potential scale should be made carefully, since there is no reference electrode in the MJ. The parallel fabrication of PPF/nitroazobenzene/Cu/Au devices is shown in figure 3, taking full advantage of the ability to pattern PPF[28].

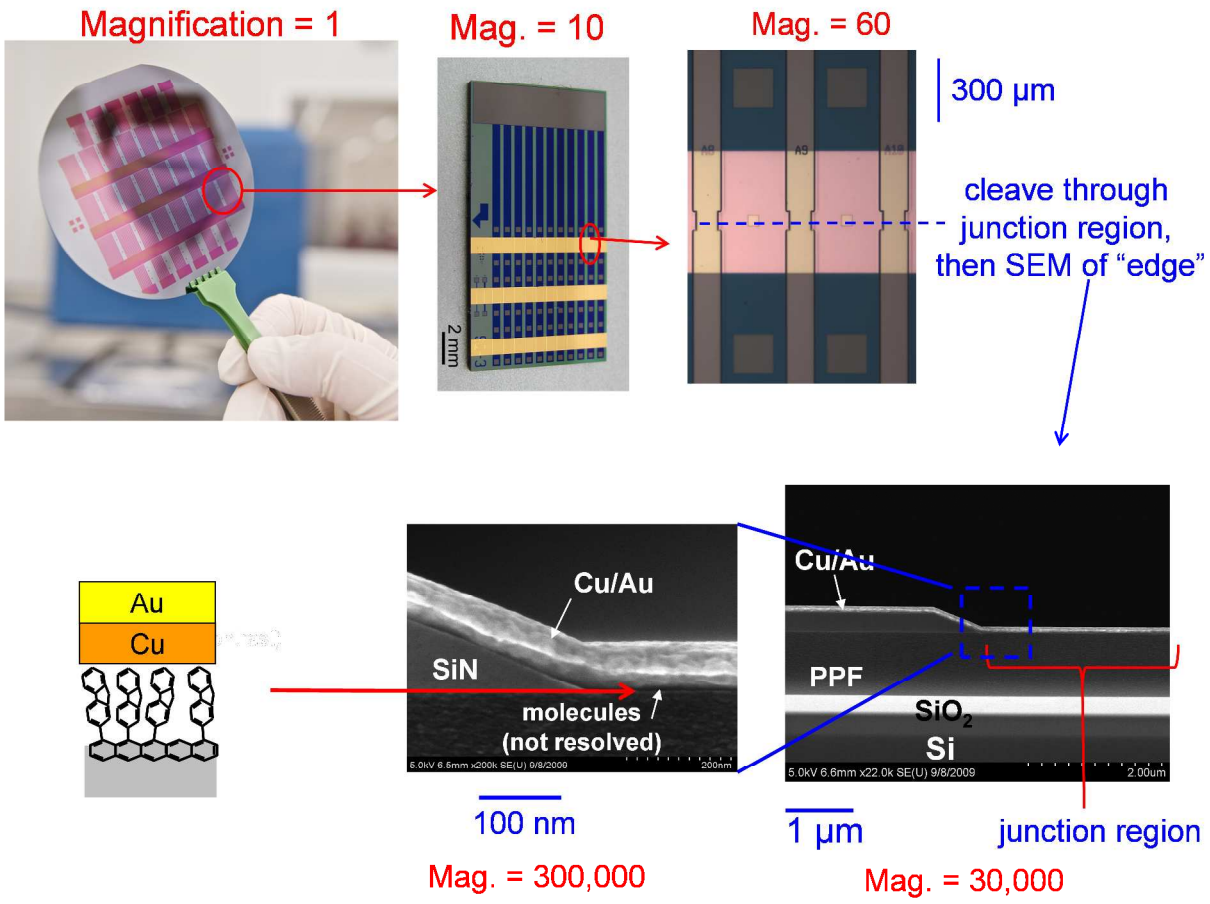


**Figure 3**. Images of fabrication steps for PPF/molecule/Cu molecular junctions from a photoresist pattern on SiOx. Increasing magnification clockwise from upper left photograph.

In the case shown, 36 "chips" can be fabricated on one 4" silicon wafer, then each chip may be modified electrochemically and have its top contact deposited to yield 32 identical MJs/chip.

Figure 4A shows the current density/voltage (*JV*) curves for all 32 junctions on one chip, obtained at 1000 V/sec, with the applied bias stated as PPF relative to Cu (i.e. PPF is +). The steep curve occurs with the molecular layer absent, due to the direct contact between the two electronic conductors (PPF and Cu). If molecules behaved like resistors and were governed by Ohm's law, a linear dashed line would be observed with its slope proportional to the inverse of the resistance. If a 3.5 nm thick layer of nitroazobenzene (NAB) is present between the PPF and

Cu, the 32 overlaid sigmoidal curves are observed, with a reproducibility of current density of 10-20% across the 32 devices. A plot of the same data on a log scale in figure 4B exhibits linear regions above ~0.2 V, indicating exponential dependence of current on applied bias.

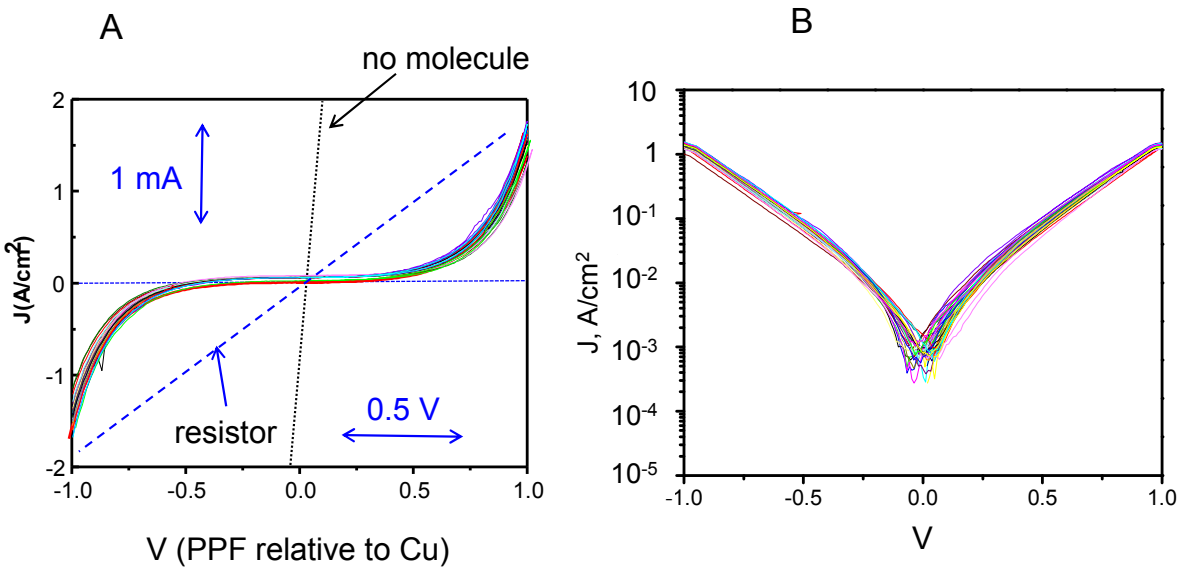


**Figure 4**. Current density (*J*) vs. voltage curves for PPF/NAB/Cu molecular junctions containing an NAB multilayer 3.5 nm thick. (A) shows an overlay of 32 curves from one "chip", compared to a device without an NAB layer. (B) is same data on a logarithmic *J* scale.

The *JV* curves are weakly dependent on temperature, with no change of shape or current density between 5K and 200K, and an Arrhenius slope of 37 meV between 250 and 350 K[29]. They were also scan rate independent, at least between 0.1 and 10,000 V/sec, except for a capacitive current observed at high scan rates. The *JV* curves were unchanged after $>10^9$ cycles to $|J| > 1$ A/cm$^2$, even at 100 $^{o}$C. We have reported extensively on the characteristics of MJs corresponding to figure 1B but with variations in molecular structure, molecular layer thickness, top contact composition, and temperature[6, 25, 29-33]. The MJ current at a particular bias is exponentially dependent on molecular layer thickness (*d*), as shown in figure 5A, and alkanes differ significantly from NAB in the slope of the ln*J* vs *d* plot, generally designated as *β,* the

attenuation coefficient, with units of $nm^{-1}$ ($Å^{-1}$ is also common). A $\beta$ of 2.5 $nm^{-1}$ indicates that the observed current density decreases by a factor of 1/e for each 0.4 nm of molecular layer thickness, while an alkane junction would show a similar attenuation with a thickness increase of 0.12 nm.

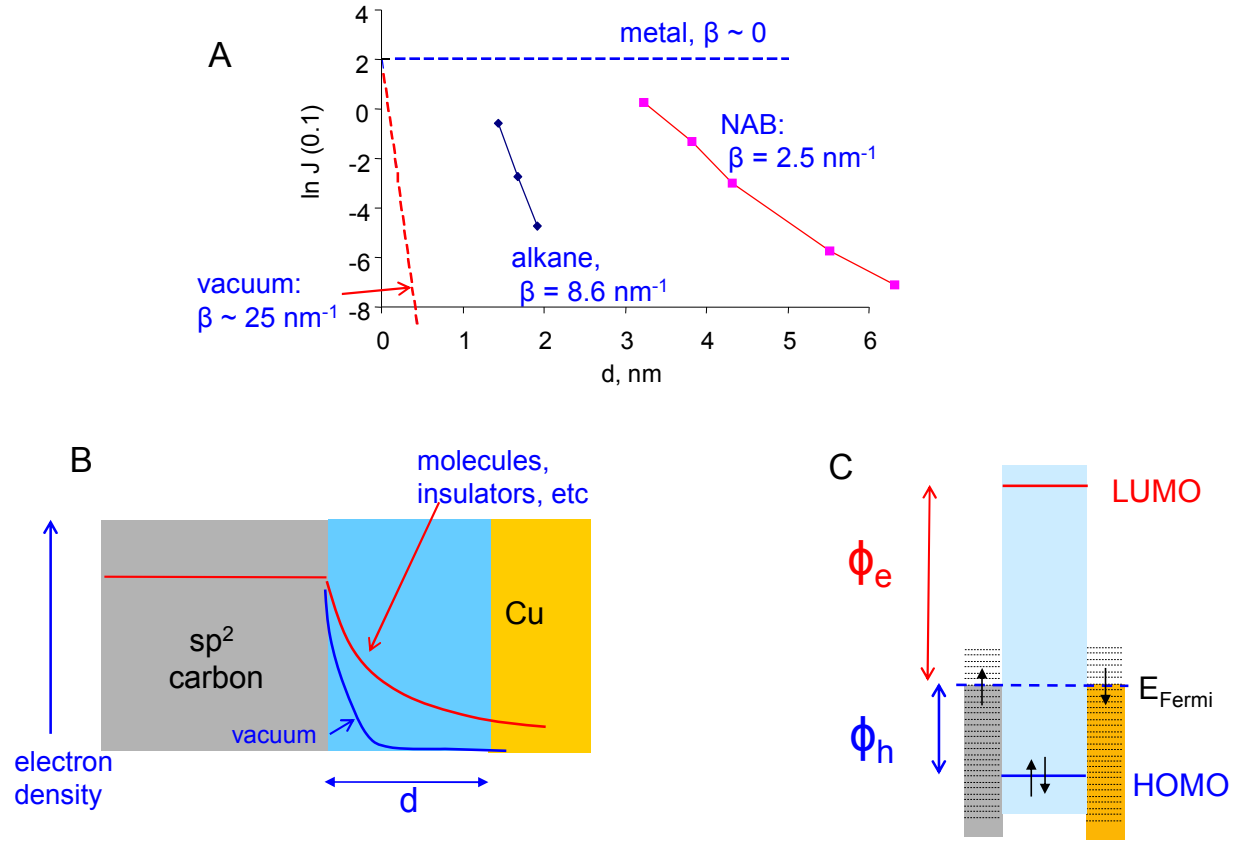


**Figure 5**. (A) Plots of ln(*J*) observed at a 0.1 V bias vs the thickness of molecules between the two conducting contacts. Dashed lines are predicted for a vacuum or metal, while experimental results for an alkane series and NAB[29, 34] are shown with their slopes. (B) Schematic of electron density distribution outside of a $sp^2$ carbon surface, with a Cu electrode positioned a distance *d* from the carbon. (C) simplified schematic of tunnelling barriers for electron ($\Phi_e$) or hole ($\Phi_h$) tunnelling across a molecular junction.

Based on a long history of electron transfer in donor-acceptor molecules and through molecular monolayers on electrodes in solution, the distance dependence observed in figure 5A and in a variety of molecular junctions has been attributed to quantum mechanical tunnelling, depicted for the current MJs in figure 5B. The electron density in the $sp^2$ carbon extends beyond

the carbon surface due to the wave-like behaviour of electrons. There is a finite probability of finding an electron at some distance ($d$) from the carbon surface, and this probability generally decreases exponentially with $d$. In a vacuum, the decrease is very rapid, with the probability decreasing by a factor of $e^{25}$ over a distance of 1 nm. However, if the vacuum is replaced by a molecule or metal oxide, the attenuation is more gradual, and $\beta$ depends on the properties of the material involved. If $d$ is small enough, there is finite overlap between the electron density from the carbon surface and the Cu contact, thus permitting electron transport across the molecular layer in response to an applied bias. Electron tunnelling with its exponential distance dependence has been reported for a wide range of systems[5, 22, 35-45], including single molecule as well as "ensemble" MJs, and it is reassuring that a $\beta$ of 8-9 $nm^{-1}$ is often reported for aliphatic molecules in homogeneous, electrochemical, and solid state electron transport.

Off- resonant tunnelling mechanisms always involve an energy barrier, with higher or thicker barriers decreasing the probability of a tunnelling event. The often assumed barriers for a MJ are shown in figure 5C, with $\Phi_e$ indicating the electron tunnelling barrier, assumed to equal the difference in energy between the Fermi level of the contacts and the lowest unoccupied molecular orbital (LUMO). An analogous but less intuitive hole tunnelling barrier, $\Phi_e$ is mediated by the highest occupied molecular orbital (HOMO). In both cases, transport would be favourable if the orbital involved were at the same energy as the Fermi level, and the displacement of the orbital energy from $E_{Fermi}$ represents the corresponding tunnelling barrier. By classical tunnelling theory, $\beta$ should be proportional to the square root of the barrier height[46-48]; hence the slope of plots such as figure 5A should depend strongly on the HOMO or LUMO levels of the molecules involved. We tested this hypothesis by making an extensive series of 400 MJs of the type shown in figure 1B, with seven aromatic structures in addition to the alkanes[22,

[34]. The aromatic molecules had structures similar to NAB, but were chosen to have a range of HOMO energies of 2.3 eV, and a range of LUMO energies of 2.7 eV. The variation in orbital energies should have caused a large variation in current density, since the barrier height occurs in the exponential portion of the tunnelling current expression. Surprisingly, the seven aromatic molecules had $\beta$ coefficients which were statistically equal ($2.7 \pm 0.6$ nm$^{-1}$), and the absolute current densities were also quite similar, indicating a barrier height for the aromatic molecules of $1.3 \pm 0.2$ eV[29, 34]. Furthermore, the insensitivity of the observed tunnelling barrier to the orbital energies of the free molecules was confirmed by ultraviolet photoelectron spectroscopy, which indicated a barrier of $1.4 \pm 0.2$ eV for the aromatic series.

This unexpected (in fact, disappointing) result is a consequence of the insufficiency of free molecule properties for predicting the behaviour of molecules bonded to one or more conductors. The Mott-Schottky limit is often used in semiconductor electronics for a case where the electronic properties of two solid phases are not perturbed significantly from their isolated states when they are put together to form an interface. In this limit, the HOMO energy of a free molecule would be the same in a MJ as in the molecule's isolated state, and the barriers depicted in figure 5C could be readily determined from the properties of the carbon electrode and the free molecule. However, if the two phases interact electronically, particularly by charge transfer across the interface, the classical literature used the terms "strong electronic coupling", also the "Bardeen limit". Such electronic interactions have been described extensively for interfaces between two semiconductors, a metal and semiconductor, or a metal and organic layer, and can result in apparent changes in work function and alterations in orbital energies of the system[43, 49-53]. Bonding an aromatic molecule to the surface of PPF creates a conjugated, covalent bond between two aromatic systems, which are likely to interact electronically. If an electron

withdrawing group is placed in the molecular layer, partial electron transfer occurs from the graphene to the molecular layer, which in turn makes the local electrostatic potential more negative. This electrostatic shift increases the energies of the HOMO or LUMO of the molecule relative to the contact Fermi level, thus decreasing $\Phi_h$ and increasing $\Phi_e$. Similarly, partial charge transfer from the molecule to the carbon causes an electronic shift in the opposite direction, increasing $\Phi_h$ and decreasing $\Phi_e$. As a result, the changes in free molecule HOMO and LUMO energies from donating or withdrawing groups are counteracted by a "levelling effect" which compresses the expected tunnelling barriers to similar values, i.e. 1.3 ± 0.2 eV. These results indicate strongly that a MJ must be treated as a complete electronic system consisting of both contacts and the molecular layer, rather than basing expectations on the properties of isolated materials.

Although the levelling effect frustrated attempts to vary tunnelling current by changes in molecular structure, it was observed for PPF/molecule/Cu devices with thicknesses less than 6 nm, in which tunnelling is the dominant transport mechanism. We next considered transport "beyond tunnelling" where MJ thickness was extended beyond 6 nm, and other transport mechanisms might be possible. Three examples are shown in figure 6, which is an attenuation plot for PPF/molecule/e-C/Au devices similar to that of figure 1B, but with e-C as the top contact and a wider thickness range.

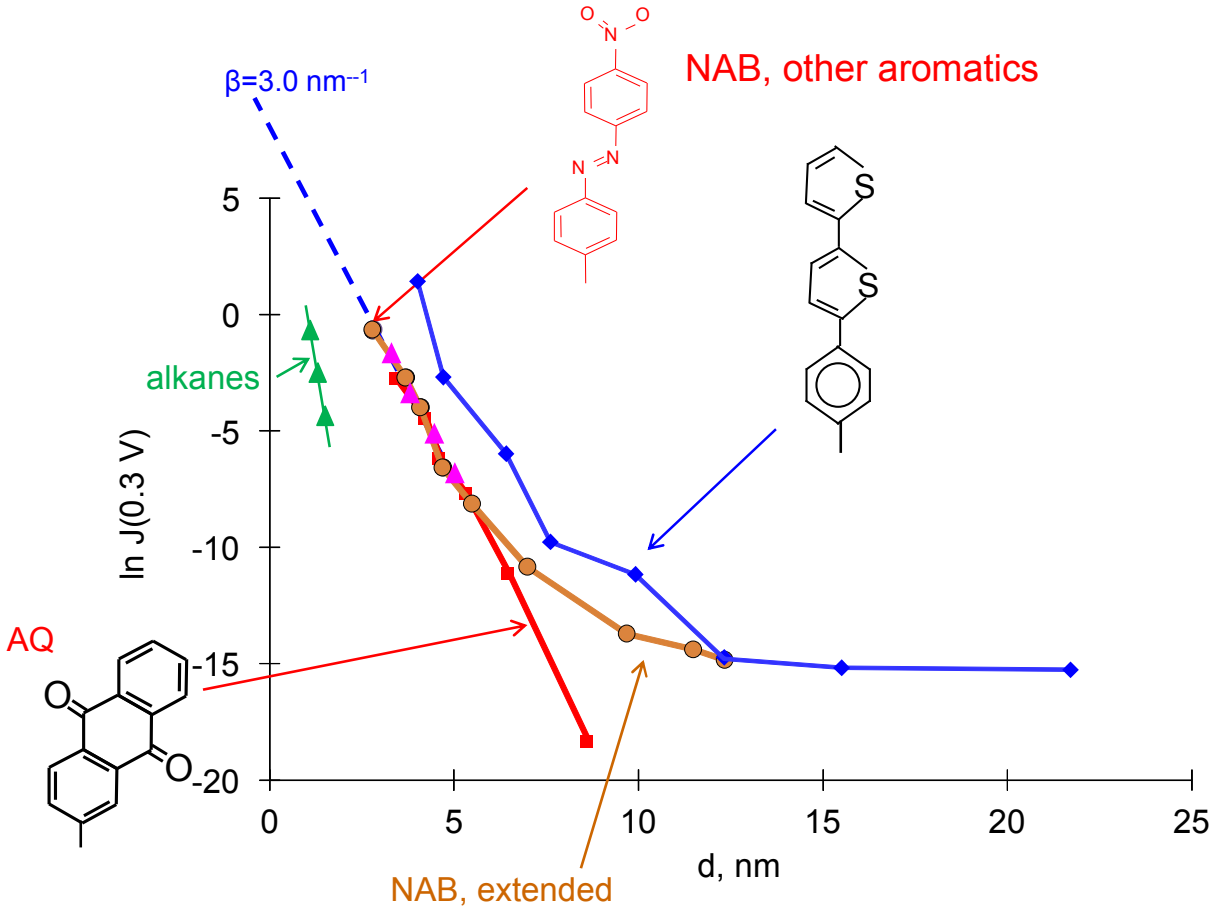


**Figure 6.** Attenuation plot of ln(*J*, 0.3 V) vs molecular layer thickness for alkanes[22], NAB, anthraquinone, and bis-thienylbenzene [30] between PPF and Cu (alkane) and e-Carbon/Au electrodes (NAB, AQ, BTB).

The alkane and aromatic devices with d < 6 nm have the same β values as the copper devices, with a similar "levelling" effect. However, extension of anthraquinone (AQ) and NAB to d > 6 nm showed some significant differences. $\beta$ for AQ remains at 3.0 $nm^{-1}$ for *d* up to 9 nm, where the current decreased below the detection limit for the 0.3 V bias. NAB exhibited curvature about 6 nm, with ~400 time higher current density than AQ for *d* =9 nm. Bisthienylbenzene (BTB) shows three regions in the attenuation plot, $\beta$ = 3 $nm^{-1}$ below *d*=8 nm, $\beta$ = 1.0 $nm^{-1}$ for *d*=8 – 13 nm, and $\beta \approx 0$ $nm^{-1}$ for *d* > 15 nm. A detailed analysis of the BTB case, including temperature dependence, concluded that three mechanisms were operative, including tunnelling

for short distance, activated hopping for $d > 15$ nm and T > 200 K, and possibly field ionization for $d = 12$-16 nm. Therefore, there are likely several transport mechanisms "beyond tunnelling", and they may have significant roles to play in practical applications of molecular electronics.

**4. Audio processing with carbon-based molecular junctions**

The tunnelling behaviour evident in figure 4A may have commercially useful properties in the near future, in a rather unexpected electronic application. Electric guitar output is often modified before amplification to improve sound quality and introduce unusual audible effects. "Analog distortion pedals" intentionally distort the guitar output to generate harmonics which are perceived as a "warmer" sound. The harmonic distribution of any musical instrument has a strong effect on its sound quality, so electronic modifications are quite common in popular music. The tunnelling behaviour of figure 4A is rarely observed in conventional silicon electronic devices, and in fact is usually avoided to reduce "leakage" current. However, the nonlinear *JV* behaviour of a MJ may be well suited for generating harmonics, using an arrangement similar to that shown in figure 7.

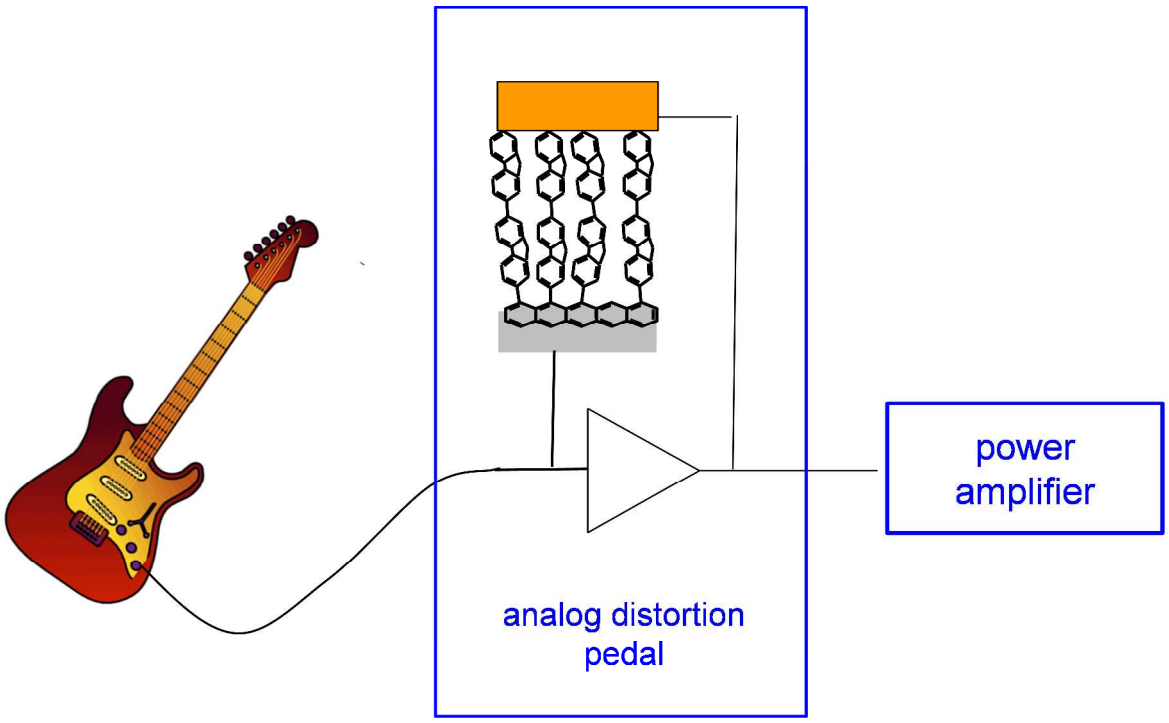


**Figure 7.** Schematic of an audio distortion circuit incorporating a molecular junction. The triangle represents the amplifier itself, which could be a transistor or operational amplifier. The distortion introduced by the molecular junction changes the harmonic distribution of the signal, thus modifying the "sound".

A MJ combined with a conventional transistor or operational amplifier introduces harmonics into the signal which are clearly audible. Since the *JV* curve in figure 4A for the MJ is not possible with silicon (to our knowledge), the distribution or harmonics should be distinct from what is currently possible. Furthermore, the MJ behaviour is easily varied by changing its thickness, so a range of distortion should be possible using different MJs, or with the associated conventional circuit components combined with an MJ. A commercial prototype of an analog distortion pedal which incorporates an "all carbon" MJ is currently under evaluation, and commercial availability is likely before the end of 2014.

## 5. Highly ordered pyrolytic graphite (HOPG) revisited

HOPG has long been used as an X-ray monochromator, due to its well-defined interplanar spacing of 3.35 Å. Following an early investigation by Randin and Yeager regarding the low double layer capacitance of HOPG [54], the electrochemical behaviour of HOPG as an electrode in solution was explored extensively starting in the 1980's[55, 56, 57, 58-60]. One motivation was to use HOPG as a structurally well-defined form of graphitic carbon as a model for widely used glassy carbon and polycrystalline graphite electrodes. As described in several reports and reviews, a general picture of what factors control the electrochemical reactivity of graphitic electrodes emerged, based on the properties of HOPG and variations in electrochemical kinetics observed at the basal and edge planes of HOPG and with a variety of surface modifications. To briefly review these conclusions, it became generally accepted that the basal plane of HOPG exhibited 3-5 orders of magnitude lower $k^o$ values for outer-sphere redox reactions such as $Ru(NH_3)_6^{+3/+2}$ and $IrCl_6^{-3/-4}$, compared to the edge plane. Certain redox systems such as aquated $Fe^{+3/+2}$ and $V^{+2/+3}$ were very sensitive to C=O groups on the carbon surface [61, 62], which rarely exist on the basal plane, if at all. Catechol oxidation was very sensitive to hydrogen bonding sites on the electrode surface, including those present during adsorption of the catechol itself. Removal of such sites nearly totally prevents catechol oxidation, and the effect was attributed to proton coupled electron transfer catalysed by surface hydrogen bonding sites [63, 64]. A related observation was that anthraquinone 2,6 disulfonate (AQDS) reduction was small or undetectable on basal plane HOPG, but strong on edge plane, leading to the proposal that AQDS adsorption occurs mainly at step edges, possibly due to the electronic disturbance introduced into the surface by defects [65-67]. The initial proposal that AQDS adsorbed solely to edge plane defects was later amended when it was observed that AQDS adsorption observed voltammetrically

corresponded to ~30 times the step edge density observable with STM[65]. This observation led to the proposal that electronic disturbances caused by step edges caused adsorption over a much larger area than the defect itself. The broad conclusion from these experiments is that HOPG basal plane is more active than edge plane regarding electrode kinetics and adsorption, but also that the nature of the kinetic heterogeneity varies significantly depending on the particular redox mechanism(s) involved[2, 68].

Subsequent reports from various laboratories using different techniques supported the generally accepted kinetic and electrochemical heterogeneity of HOPG, including electrochemical deposition of metals at step edges[69, 70], Raman spectroscopy of enhanced adsorption at edge sites[71], faster electrode kinetics at edge sites compared to basal plane[72-79], enhanced electrochemiluminescence at edge plane[59], and nucleation of diazonium derived phenyl radicals at step edges[13]. However, the advent of scanning electrochemical microscopy (SECM) and scanning electrochemical cell microscopy (SECCM) permitted monitoring electrode activity on a microscopic scale, and some of the results challenged the accepted model. In particular, "close to reversible" kinetics for $Fe(CN)_6^{-3/-4}$ and other outer sphere systems were reported on HOPG basal plane[80] using SECCM, in contrast to the very slow kinetics ($\Delta E_p$ >700 mV for $Fe(CN)_6^{-3/-4}$) reported previously on "validated" HOPG basal plane surfaces [66, 67]. The widely studied catechol dopamine was reported to have very slow kinetics on basal plane HOPG using macroscopic voltammetry [58], but later reports using SECM [81] and SECCM[82-84] reported fast kinetics on "pristine" basal plane HOPG. Furthermore, the observed electrode kinetics and AQDS adsorption on basal plane HOPG were claimed to be independent of the grade of HOPG or the density of step edges [83, 85], leading to the conclusion that defects were not controlling the observed electrochemical behaviour. A more detailed review of the many reported

electrochemical results reported on HOPG basal plane is beyond the scope of the present article, but suffice it to say that there are two incompatible viewpoints: one that basal plane HOPG has low reactivity for outer sphere electron transfer reactions, anthraquinone adsorption, and dopamine oxidation provided there is a low density of defects; and a second that such processes occur rapidly on basal plane HOPG and are not affected by step edges or other defects.

The discrepancy between macroscopic and microscopic observations on basal plane HOPG stimulated a brief reconsideration of $Fe^{+2/+3}$ kinetics in the authors' laboratory, almost two decades after the original reports [61, 62]. Using the "low defect" HOPG which is not available commercially, a series of cleaved surfaces were examined with voltammetry of 1 mM $Fe^{+2/+3}$ in 1 M $HClO_4$, using the "inverted drop" cell to avoid mechanical strain on the sample. The experiments were done using ultrapure water (18 MΩ, < 10 ppb TOC), with less than 1 minute exposure of the cleaved surfaces to air, in a different lab (and different country) from the 1990's experiments, with the results shown in figure 8. The inverted drop area was not controlled, producing the variation in peak current, but the electrode kinetics clearly vary significantly for surfaces cleaved by different methods. When the cleaving method prescribed in 1992[67] was used repeatedly, four successive cleaves produced $\Delta E_p > 1000$ mV for $Fe^{+2/+3}$.

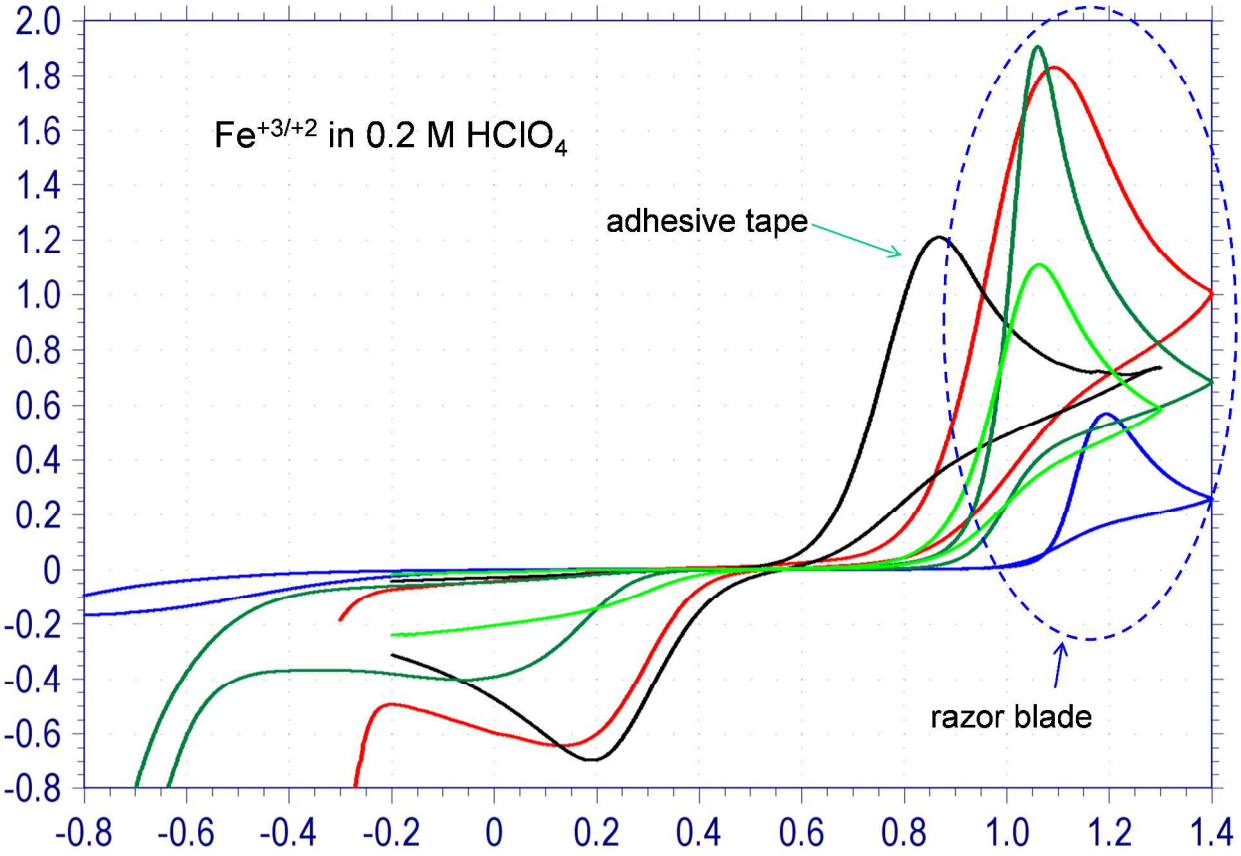


**Figure 8.** Cyclic voltammograms (0.2 V/s) on five basal plane HOPG surfaces obtained from the same HOPG sample with various cleaving techniques, including removal of several layers using adhesive tape. Solution contained $Fe^{+3/+2}$ in 0.2 M $HClO_4$ in ultrapure water (18 MΩ resistivity, TOC< 10 ppb), and was placed on the HOPG surface as an inverted drop with uncontrolled diameter within one minute of cleaving the sample in air. The blue curve showing the largest $\Delta E_p$ was obtained with the technique used previously [66, 67], the green and red curves by a razor blade inserted between graphite layers to expose a cleaved surface.

There are at least two possible reasons for a scientific disagreement, a problem with the experimental results or a difference in interpretation. An example of the latter is the proposal that step edges or defects and their effects on the density of electronic states are responsible for certain electrochemical behaviour on HOPG, such as adsorption or faster electron transfer kinetics. The complexity of the electronic and chemical properties of carbon materials in their variety of allotropes and crystallinity will undoubtedly result in variations in behaviour, and it will be a long time before the underlying materials properties which determine electrochemical

reactivity are fully understood. However, the discrepancy regarding HOPG basal plane reactivity is more fundamental, in that different laboratories have reported many results at opposite extremes, e.g., from "very slow" to "reversible" in the case of electrode kinetics of $Fe(CN)_6^{-3/-4}$. Several established laboratories report discordant results using similar experimental conditions, in some cases even the same source of HOPG. Obviously, since the interpretation and any scientific conclusions are based on experimental results, it is difficult to proceed if those results differ as much as claimed for HOPG basal plane electrochemistry.

Our early conclusion that HOPG surfaces varied significantly in defect density was based on the experimental observation of adsorption, capacitance, and $\Delta E_p$ ($Fe(CN)_6^{-3/-4}$, 1 V/sec) for a series of HOPG surfaces. For the ungraded or highest commercial grades available at the time, the AQDS capacitance varied from < 1 to 69 pmol/cm$^2$, the capacitance from 0.6 to 6.5 μF.cm$^2$, and $\Delta E_p$ from 92 to >1000 mV [67]. Therefore, we selected surfaces for closer study which had the lowest adsorption and largest $\Delta E_p$ as being the most representative of low-defect HOPG basal plane behaviour. Recall that HOPG is far from a single crystal, with both a finite in-plane microcrystallite size (~a few μm) and "turbostratic" disorder, with crystallites rotated relative to each other around the axis perpendicular to the basal plane surface. The effect of such disorder on electronic properties is an active and complex research area, and will likely remain so for a long time. Step edges or other defects may have a large effect on electronic properties, through changes in density of electronic states, scattering centres, grain boundaries, etc. Suppose that these electronic disturbances underlie the variation in electron transfer rate and adsorption, and that the electronic changes depend strongly on defects. Since catechols can be "self-catalyzed" by their own adsorption and subsequent proton coupled electron transfer [63, 64], a defective surface would appear reactive once catechol (or its quinone) adsorption occurs. Furthermore, Ta and

McDermott[86] reported that using voltammetry to measure AQDS adsorption may be complicated by the interaction of both adsorption itself and the varying electrochemical reactivity near defects. As an indication of the strong electronic consequences of defects, consider the example of basal plane graphite modified by chemisorption of H atoms, to form single $sp^3$ point defects in an otherwise $sp^2$ hybridized surface[87]. STM in a UHV environment revealed a "charge redistribution" which extended ~5 nm away from the point defect, corresponding to an area of ~78 $nm^2$. Taking the carbon number density as 3.8 x $10^{15}$ $cm^{-2}$ [88], there are ~3000 carbon atoms in the surface graphene layer within 5 nm of the $sp^3$ centre. Stated differently, ~2 x $10^{-12}$ $mol/cm^2$ of defects would result in charge redistribution of the *entire* basal surface. Such electronic perturbations do not necessary result in changes in adsorption or electrode kinetics, but they do indicate the sensitivity of basal plane HOPG to a low density of defects. As pointed out in early reports, mechanical strain (e.g. from adhesive tape) during cleaving significantly reduced the probability of obtaining a low defect surface[67].

The discussion about the electrochemical reactivity of basal plane HOPG will likely continue for some time, given the disparity in experimental results. The only way this author can explain such disparity is by invoking electronic disturbances which vary with the source of HOPG and the history of each individual basal surface. Without some type of "selection" procedure, the results can vary greatly, using the same sample and identical procedure. Either the "selection" procedure is fundamentally flawed, or there are possibly unknown characteristics of HOPG which are not captured in a simple, crystalline model, and are not controlled experimentally.

**Future Perspectives:**

It is clearly evident from the many interesting papers and associated discussion in this volume that the electrochemistry and electronic properties of carbon materials remain active research fields even after many decades of modern research. The advent of fullerenes, particularly carbon nanotubes and graphene, have rekindled the already active research on electrochemistry at carbon electrodes. Nearly all of the allotropes of elements other than carbon have been known for more than a century, yet a new allotrope of carbon was discovered in 1985, and a vast new research area emerged as a result. The combination of a metallic or semiconducting solid material with the rich covalent chemistry of carbon underlie both the attractive electrochemical properties of carbon materials as well as their application in solid state molecular electronic devices. The widespread applications of carbon electrodes described in this Faraday Discussion range from nanoscale phenomena at interfaces in both solution and solid state to large scale industrial applications in supercapacitors and electrocatalysis. Like many vibrant areas of scientific research, our current knowledge of the electronic and electrochemical behaviour of carbon materials is really the "tip of the iceberg", and the possibilities for future development are both extensive and intriguing.

**Acknowledgements**

This work was supported by Natural Sciences and Engineering Research Council of Canada, the National Institute for Nanotechnology, The University of Alberta, and The Province of Alberta. The National Institute for Nanotechnology is operated as a partnership between the National Research Council and the University of Alberta and is jointly funded by the Government of Canada, the Government of Alberta, and the University of Alberta. Research

from the authors' laboratory preceding 2006 was funded by the National Science Foundation (USA), the Air Force Office of Scientific Research (USA) and Ohio State University.

**References**

1. R. L. McCreery, in *Electroanalytical Chemistry*, ed. A. J. Bard, Dekker, N.Y., 1991, vol. 17, pp. 221-374.
2. R. L. McCreery, *Chem. Rev.*, 2008, 108, 2646-2687.
3. D. Belanger and J. Pinson, *Chem. Soc. Rev.*, 2011, 40, 3995-4048.
4. J. Pinson and F. Podvorica, *Chem. Soc. Rev.*, 2005, 34, 429-439.
5. R. L. McCreery and A. J. Bergren, *Adv. Mater.*, 2009, 21, 4303-4322.
6. R. McCreery, J. Wu and R. J. Kalakodimi, *Phys. Chem. Chem. Phys.*, 2006, 8, 2572-2590.
7. T.-C. Kuo, Ph.D. thesis, The Ohio State University, 1999.
8. R. Kostecki, B. Schnyder, D. Alliata, X. Song, K. Kinoshita and R. Kotz, *Thin Solid Films*, 2001, 396, 36-43.
9. R. Kostecki, X. Song and K. Kinoshita, *Electrochemical and Solid-State Letters*, 1999, 2, 465-467.
10. S. Ranganathan and R. L. McCreery, *Anal. Chem.*, 2001, 73, 893-900.
11. S. Ranganathan, R. L. McCreery, S. M. Majji and M. Madou, *J. Electrochem. Soc,*, 2000, 147, 277 - 282.
12. J. K. Kariuki and M. T. McDermott, *Langmuir*, 2001, 17, 5947-5951.
13. J. K. Kariuki and M. T. McDermott, *Langmuir*, 1999, 15, 6534-6540.
14. F. Anariba, S. H. DuVall and R. L. McCreery, *Anal. Chem.*, 2003, 75, 3837-3844.
15. P. Allongue, M. Delamar, B. Desbat, O. Fagebaume, R. Hitmi, J. Pinson and J. M. Saveant, *J. Am. Chem. Soc.*, 1997, 119, 201-207.
16. P. M. Kirkman, A. G. Güell, A. S. Cuharuc and P. R. Unwin, *J. Am. Chem. Soc.*, 2013, 136, 36-39.
17. T. P. DeAngelis, R. W. Hurst, A. M. Yacynych, H. B. Mark, Jr., W. R. Heineman and J. S. Mattson, *Anal. Chem.*, 1977, 49, 1395-1398.
18. J. S. Mattson and C. A. Smith, *Anal. Chem.*, 1975, 47, 1122-1125.
19. J. J. Blackstock, A. A. Rostami, A. M. Nowak, R. L. McCreery, M. Freeman and M. T. McDermott, *Anal. Chem.*, 2004, 76, 2544-2552.
20. H. Yan, A. J. Bergren and R. L. McCreery, *J. Am. Chem. Soc.*, 2011, 133, 19168-19177.
21. A. P. Bonifas and R. L. McCreery, *Nano Lett.*, 2011, 11, 4725-4729.
22. A. P. Bonifas and R. L. McCreery, *Nat. Nanotechnol.*, 2010, 5, 612-617.
23. A. M. Mahmoud, A. J. Bergren and R. L. McCreery, *Anal. Chem.*, 2009, 81, 6972-6980.
24. S. Ssenyange, H. Yan and R. L. McCreery, *Langmuir*, 2006, 22, 10689-10696.
25. R. McCreery, H. Yan and A. J. Bergren, *Phys. Chem. Chem. Phys.*, 2013, 15, 1065-1081.
26. F. Anariba, J. Steach and R. McCreery, *J. Phys. Chem. B*, 2005, 109, 11163-11172.
27. A. J. Bard and L. R. Faulkner, *Electrochemical Methods*, Wiley, New York, 2nd Edition edn., 2001.
28. J. Ru, B. Szeto, A. Bonifas and R. L. McCreery, *ACS Appl. Mater. Interfaces*, 2010, 2, 3693-3701.

29. A. J. Bergren, R. L. McCreery, S. R. Stoyanov, S. Gusarov and A. Kovalenko, *J. Phys. Chem. C*, 2010, 114, 15806-15815.
30. H. Yan, A. J. Bergren, R. McCreery, M. L. Della Rocca, P. Martin, P. Lafarge and J. C. Lacroix, *Proc. Natl. Acad. Sci.*, 2013, 110, 5326-5330.
31. S. Y. Sayed, A. Bayat, M. Kondratenko, Y. Leroux, P. Hapiot and R. L. McCreery, *J. Am. Chem. Soc.*, 2013, 135, 12972-12975.
32. J. A. Fereiro, R. L. McCreery and A. J. Bergren, *J. Am. Chem. Soc.*, 2013, 135, 9584-9587.
33. A. M. Mahmoud, A. J. Bergren, N. Pekas and R. L. McCreery, *Adv. Funct. Mater.*, 2011, 21, 2273-2281.
34. S. Y. Sayed, J. A. Fereiro, H. Yan, R. L. McCreery and A. J. Bergren, *Proc. Natl. Acad. Sci.*, 2012, 109, 11498-11503.
35. S. M. Lindsay and M. A. Ratner, *Adv. Mater.*, 2007, 19, 23-31.
36. H. T. Nicolai, M. Kuik, G. A. H. Wetzelaer, B. de Boer, C. Campbell, C. Risko, J. L. Bredas and P. W. M. Blom, *Nature Materials*, 2012, 11, 882-887.
37. P. A. Van Hal, E. C. P. Smits, T. C. T. Geuns, H. B. Akkerman, B. C. De Brito, S. Perissinotto, G. Lanzani, A. J. Kronemeijer, V. Geskin, J. Cornil, P. W. M. Blom, B. De Boer and D. M. De Leeuw, *Nat. Nanotechnol.*, 2008, 3, 749-754.
38. H. B. Akkerman and B. De Boer, *J. Phys.: Condens. Matter*, 2008, 20, 013001.
39. H. B. Akkerman, R. C. G. Naber, B. Jongbloed, P. A. van Hal, P. W. M. Blom, D. M. de Leeuw and B. de Boer, *Proc. Natl. Acad. Sci.*, 2007, 104, 11161-11166.
40. L. Luo, S. H. Choi and C. D. Frisbie, *Chem Mater.*, 2011, 23, 631-645.
41. S. H. Choi, C. Risko, M. C. R. Delgado, B. Kim, J.-L. Bredas and C. D. Frisbie, *J. Am. Chem. Soc.*, 2010, 132, 4358-4368.
42. S. H. Choi, B. Kim and C. D. Frisbie, *Science*, 2008, 320, 1482-1486.
43. O. Yaffe, Y. B. Qi, L. Scheres, S. R. Puniredd, L. Segev, T. Ely, H. Haick, H. Zuilhof, A. Vilan, L. Kronik, A. Kahn and D. Cahen, *Phys. Rev. B*, 2012, 85, 045433.
44. A. Vilan, O. Yaffe, A. Biller, A. Salomon, A. Kahn and D. Cahen, *Adv. Mater.*, 2010, 22, 140-159.
45. I. Ron, I. Pecht, M. Sheves and D. Cahen, *Acc. Chem. Res.*, 2010, 43, 945-953.
46. J. G. Simmons, *J. Appl. Phys.*, 1964, 35, 2655-2658.
47. J. G. Simmons, *J. Appl. Phys.*, 1963, 34, 2581-2590.
48. J. G. Simmons, *J. Appl. Phys.*, 1963, 34, 1793-1803.
49. J. Hwang, A. Wan and A. Kahn, *Materials Science and Engineering: R: Reports*, 2009, 64, 1-31.
50. A. Salomon, T. Boecking, O. Seitz, T. Markus, F. Amy, C. Chan, W. Zhao, D. Cahen and A. Kahn, *Adv. Mater.*, 2007, 19, 445-450.
51. D. Cahen, A. Kahn and E. Umbach, *Mater. Today*, 2005, 8, 32-41.
52. F. Li, Y. Zhou, F. Zhang, X. Liu, Y. Zhan and M. Fahlman, *Chem Mater.*, 2009, 21, 2798-2802.
53. C. Tengstedt, W. Osikowicz, W. R. Salaneck, I. D. Parker, C.-H. Hsu and M. Fahlman, *Appl. Phys. Lett.*, 2006, 88, 053502.
54. J.-P. Randin and E. Yeager, *J. Electroanal. Chem.*, 1972, 36, 257-276.
55. H. Gerischer, *J. Phys. Chem.*, 1985, 89, 4249-4251.
56. H. Gerischer, R. McIntyre, D. Scherson and W. Storck, *J. Phys. Chem.*, 1987, 91, 1930.

57. R. McIntyre, D. Scherson, W. Storck and H. Gerischer, *Electrochim. Acta*, 1987, 32, 51-53.
58. R. J. Bowling, R. T. Packard and R. L. McCreery, *J. Am. Chem. Soc.*, 1989, 111, 1217-1223.
59. R. J. Bowling, R. L. McCreery, C. M. Pharr and R. C. Engstrom, *Anal. Chem.*, 1989, 361, 2763-2766.
60. R. Bowling, R. T. Packard and R. L. McCreery, *Langmuir*, 1989, 5, 683.
61. P. Chen, M. Fryling and R. L. McCreery, *Anal. Chem.*, 1995, 67, 3115.
62. C. A. McDermott, K. Kneten and R. L. McCreery, *J. Electrochem. Soc,*, 1993, 140, 2593.
63. S. DuVall and R. L. McCreery, *J. Am. Chem. Soc.*, 2000, 122, 6759 - 6764.
64. S. DuVall and R. L. McCreery, *Anal. Chem.*, 1999, 71, 4594-4602.
65. M. T. McDermott and R. L. McCreery, *Langmuir*, 1994, 10, 4307.
66. K. K. Cline, C. A. McDermott and R. L. McCreery, *J. Phys. Chem.*, 1994, 98, 5314.
67. M. T. McDermott, K. Kneten and R. L. McCreery, *J. Phys. Chem.*, 1992, 96, 3124.
68. R. L. McCreery and M. T. McDermott, *Anal. Chem.*, 2012, 84, 2602-2605.
69. E. C. Walter, B. J. Murray, F. Favier, G. Kaltenpoth, M. Grunze and R. M. Penner, *J. Phys. Chem. B*, 2002, 106, 11407-11411.
70. R. M. Penner, M. J. Heben, T. L. Longin and N. S. Lewis, *Science*, 1990, 250, 1118-1121.
71. K. G. Ray and R. L. McCreery, *Anal. Chem.*, 1997, 69, 4680-4687.
72. T. J. Davies, M. E. Hyde and R. G. Compton, *Angew. Chem. Int. Ed.*, 2005, 44, 5121-5126.
73. R. R. Moore, C. E. Banks and R. G. Compton, *Anal. Chem.*, 2004, 76, 2677-2682.
74. T. J. Davies, R. R. Moore, C. E. Banks and R. G. Compton, *J. Electroanal. Chem.*, 2004, 574, 123-152.
75. C.-Y. Lee and A. M. Bond, *Anal. Chem.*, 2009, 81, 584-594.
76. F. Armstrong, A. Bond, H. Hill, I. Psalti and C. Zoski, *J. Phys. Chem.*, 1989, 93, 6485-6493.
77. F. Armstrong, A. Bond, H. Hill, N. Oliver and I. Psalti, *J. Am. Chem. Soc.*, 1989, 111, 9185-9189.
78. N. L. Ritzert, J. Rodríguez-López, C. Tan and H. D. Abruña, *Langmuir*, 2013, 29, 1683-1694.
79. W. Li, C. Tan, M. A. Lowe, H. D. Abruna and D. C. Ralph, *ACS Nano*, 2011, 5, 2264-2270.
80. S. C. S. Lai, A. N. Patel, K. McKelvey and P. R. Unwin, *Angew. Chem. Int. Ed.*, 2012, 51, 5405-5408.
81. S. Lhenry, Y. R. Leroux and P. Hapiot, *Anal. Chem.*, 2012, 84, 7518-7524.
82. A. N. Patel, K. McKelvey and P. R. Unwin, *J. Am. Chem. Soc.*, 2012, 134, 20246-20249.
83. A. N. Patel, S.-y. Tan, T. S. Miller, J. V. Macpherson and P. R. Unwin, *Anal. Chem.*, 2013, 85, 11755-11764.
84. A. N. Patel, S.-y. Tan and P. R. Unwin, *Chem. Commun.*, 2013, 49, 8776-8778.
85. G. Zhang, P. M. Kirkman, A. N. Patel, A. S. Cuharuc, K. McKelvey and P. R. Unwin, *J. Am. Chem. Soc.*, 2014, 136, 11444-11451.
86. T. C. Ta, V. Kanda and M. T. McDermott, *J. Phys. Chem. B*, 1999, 103, 1295-1302.
87. P. Ruffieux, M. Melle-Franco, O. Gröning, M. Bielmann, F. Zerbetto and P. Gröning, *Phys. Rev. B*, 2005, 71, 153403.

88. N. Jung, A. C. Crowther, N. Kim, P. Kim and L. Brus, *ACS Nano*, 2010, 4, 7005-7013.